

SepViT: Separable Vision Transformer

Wei Li^{1,2†*}, Xing Wang^{2*}, Xin Xia², Jie Wu², Xuefeng Xiao²,
Min Zheng², and Shiping Wen³

¹ University of Electronic Science and Technology of China

² ByteDance Inc.

³ University of Technology Sydney

Abstract. Vision Transformers have witnessed prevailing success in a series of vision tasks. However, they often require enormous amount of computations to achieve high performance, which is burdensome to deploy on resource-constrained devices. To address these issues, we draw lessons from depthwise separable convolution and imitate its ideology to design the Separable Vision Transformer, abbreviated as SepViT. SepViT helps to carry out the information interaction within and among the windows via a depthwise separable self-attention. The novel window token embedding and grouped self-attention are employed to model the attention relationship among windows with negligible computational cost and capture a long-range visual dependencies of multiple windows, respectively. Extensive experiments on various benchmark tasks demonstrate SepViT can achieve state-of-the-art results in terms of trade-off between accuracy and latency. Among them, SepViT achieves 84.0% top-1 accuracy on ImageNet-1K classification while decreasing the latency by 40%, compared to the ones with similar accuracy (e.g., CSWin, PVT-V2). As for the downstream vision tasks, SepViT with fewer FLOPs can achieve 50.4% mIoU on ADE20K semantic segmentation task, 47.5 AP on the RetinaNet-based COCO detection task, 48.7 box AP and 43.9 mask AP on Mask R-CNN-based COCO detection and segmentation tasks.

Keywords: Separable Vision Transformer, Depthwise Separable Self-Attention, Grouped Self-Attention, Window Token Embedding.

1 Introduction

In recent years, many computer vision (CV) researchers make efforts to design CV-oriented vision Transformer to surpass the performance of the convolutional neural networks (CNNs). Due to a high capability in modeling the long-range dependencies, vision Transformer achieves prominent results in diversified vision tasks, such as image classification [9,32,12,23,5,8], semantic segmentation [38,44,33], object detection [1,46,7] and etc. However, the powerful performance usually comes at a cost of heavy computational complexity.

* Corresponding Authors. †Intern at ByteDance.

Email: weili@std.uestc.edu.cn, wangxing.613@bytedance.com

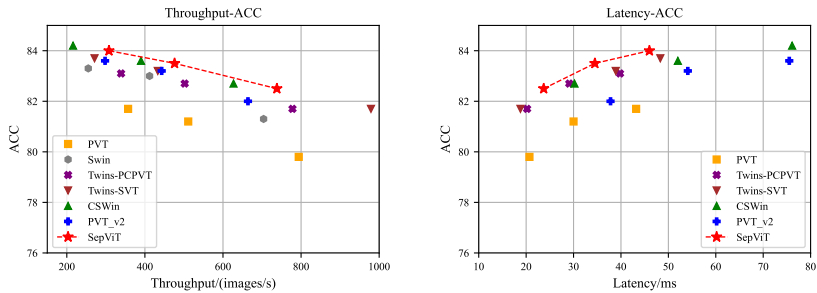


Fig. 1. Comparison of throughput and latency on ImageNet-1K classification. The throughput and the latency are tested based on the PyTorch framework with a V100 GPU and TensorRT framework with a T4 GPU, respectively.

Primordially, ViT [9] firstly introduces Transformer to the image recognition tasks. It splits the whole image into patches and feeds each patch as a token into Transformer. However, the patch-based Transformer is hard to deploy due to the computationally inefficient full-attention mechanism. To relieve this problem, Swin [23] proposes the window-based self-attention to limit the computation of self-attention in non-overlapping sub-windows. Obviously, the window-based self-attention helps to reduce the complexity to a great extent, but the shifted operator for building connection among the windows brings difficulty for ONNX or TensorRT deployment. Twins [5] takes advantage of the window-based self-attention and the spatial reduction attention from PVT [35] and proposes the spatially separable self-attention. Although Twins is deployment-friendly and achieves outstanding performance, its computational complexity is hardly reduced. CSWin [8] shows state-of-the-art performance via the novel cross-shaped window self-attention, but its throughput is low. Albeit, with varying degrees of progress in these famous vision Transformers, most of its recent successes are accompanied with huge resource demands.

To overcome the aforementioned issues, we propose an efficient Transformer backbone, called **Separable Vision Transformer (SepViT)**, which captures both local and global dependencies in a sequential order. A key design element of SepViT is its **depthwise separable self-attention** module, as shown in Fig. 2. Inspired by the depthwise separable convolution in MobileNets [16,29,15], we re-design the self-attention module and propose the depthwise separable self-attention, which consists of a depthwise self-attention and a pointwise self-attention that can correspond to depthwise and pointwise convolution in MobileNets, respectively. The depthwise self-attention is used to capture local feature within each window while the pointwise self-attention is for building connections among windows that notably improve the expressive power. Moreover, to get the global representation of a local window, we develop a novel **window token embedding**, which can model the attention relationship among windows with negligible cost. Furthermore, we also extend the idea of grouped convolu-

tion from AlexNet [19] to our depthwise separable self-attention and present the **grouped self-attention** to further improve the performance.

To demonstrate the effectiveness of SepViT, we conduct a series of experiments on some typical vision tasks, including ImageNet-1K [28] classification, ADE20K [45] semantic segmentation and COCO [22] object detection and instance segmentation. The experimental results show that SepViT can achieve a better trade-off between performance and latency than other competitive vision Transformers [35,23,5,8]. As shown in Fig. 1, SepViT achieves better accuracy at the same latency constraint and costs less inference time than the methods with the same accuracy. Furthermore, SepViT can be expediently applied and deployed since it only contains some universal operators (e.g., transpose and matrix multiplication). To sum up, the contributions of our work can be summarized as follows:

1. We propose the Separable Vision Transformer (SepViT) with a depthwise separable self-attention. It can achieve local information communication within the windows and global information exchange among the windows in a single Transformer block.
2. We propose the window token embedding to learn a global feature representation of each window, which helps SepViT to model the attention relationship among windows with negligible computational cost.
3. We extend depthwise separable self-attention to grouped self-attention in SepViT. It can capture more contextual concepts across multiple windows and achieve better performance.

2 Related work

2.1 Vision Transformer

In the computer vision field, CNN has been dominant for decades due to its advantages of the spatial inductive biases. Later, in order to model the global dependencies of pixels, ViT [9] introduces Transformer to computer vision for the first time and achieves an excellent performance on image classification task. In quick succession, a series of vision Transformers have been produced based on ViT. DeiT [32] introduces the knowledge distillation scheme and proposes the data-efficient image Transformer. T2T-ViT [42] progressively structurizes the image to tokens by recursively aggregating neighboring tokens into one token. TNT [12] proposes the inner and outer Transformers to model the relationship of the word embeddings and the sentence embeddings, respectively. CPVT [6] produces the conditional position encoding which is conditioned on the local neighborhood of input tokens and is adaptable to arbitrary input sizes.

Recently, PVT [35] and Swin [23] synchronously propose the hierarchical architecture which is friendly for the dense prediction tasks, such as object detection, semantic and instance segmentation. Meanwhile, Swin [23] as a pioneer proposes the window-based self-attention to compute attention within local windows. Soon after, Twins [5] and CSWin [8] sequentially propose the spatial

separable self-attention and cross-shaped window self-attention based on the hierarchical architecture. On the other hand, some researchers incorporate the spatial inductive biases of CNNs into Transformer. CoaT [40], CVT [36] and LeViT [10] introduce the convolutions before or after self-attentions and obtain well-pleasing results. Regarding to the design of lightweight Transformer, MobileFormer [4] and MobileViT [26] combine Transformer blocks with the inverted bottleneck blocks in MobileNet-V2 [29] in series and parallel. Besides, another direction of research [30,3,2,20] is to automatically search the structure details of Transformer with neural architecture search [47,41] technology.

2.2 Lightweight Convolutions

Many lightweight and mobile-friendly convolutions are proposed for mobile vision tasks. Of these, grouped convolution is the first to be proposed by AlexNet [19], which groups the feature maps and conducts the distributed training. Then the representative work of mobile-friendly convolution must be the MobileNets [16,29,15] with depthwise separable convolution. The depthwise separable convolution contains a depthwise convolution for spatial information communication and a pointwise convolution for information exchange across the channels. As time goes on, plenty of variants based on the aforementioned works are developed, such as [43,25,31,11]. In our work, we adapt the ideology of depthwise separable convolution to Transformer, which aims to reduce the Transformer’s computational complexity without the sacrifice of performance.

3 Methodology: SepViT

In this section, we first illustrate the design overview for SepViT, and then discuss some key modules within the SepViT block. Finally, we provide the architecture specifications and variants with different FLOPs.

3.1 Overview

As illustrated in Fig. 2, SepViT follows the widely-used hierarchical architecture [35,23,5,8] and the window-based self-attention [23]. Besides, SepViT also employs conditional position encoding (CPE) from [6,5]. For each stage, there is an overlapping patch merging layer for feature map downsampling followed by a series of SepViT blocks. The spatial resolution will be progressively reduced by $32\times$ with either stride 4 or 2, and the channel dimension will be doubled stage by stage. It is worth noting that both local contextual concepts and global abstraction can be captured in a single SepViT block, while other works [23,5] should employ two successive blocks to accomplish this local-global modeling. In the SepViT block, local information communication within each window is achieved by depthwise self-attention (DWA), and global information exchange among the windows is performed via pointwise self-attention (PWA).

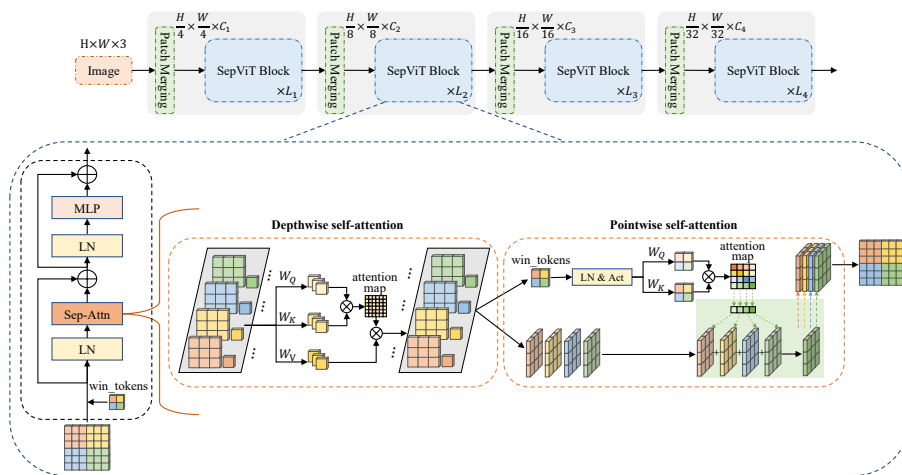


Fig. 2. Separable Vision Transformer (SepViT). The top row is the overall hierarchical architecture of SepViT. The bottom row is the SepViT block and the detailed visualization of our depthwise separable self-attention and the window token embedding scheme.

3.2 Depthwise Separable Self-Attention

Depthwise Self-Attention (DWA). Similar to some pioneering works [23,5], SepViT is built on top of the window-based self-attention scheme. Firstly, we perform a window partition on the input feature map. Each window can be seen as an input channel of the feature map, while different windows contain diverse information. Different from previous works, we create a window token for each window, which serves as a global representation and is used to model the attention relationship in the following pointwise self-attention module.

Then, a depthwise self-attention (DWA) is performed on all the pixel tokens within each window as well as its corresponding window token. This window-wise operation is quite similar to a depthwise convolution layer in MobileNets, aiming to fuse the spatial information within each channel. The implementation of DWA can be summarized as follows:

$$\text{DWA}(z) = \text{Attention}(z \cdot W_Q, z \cdot W_K, z \cdot W_V) \quad (1)$$

where z is the feature tokens, consisted of the pixel and window tokens. W_Q , W_K , and W_V denote three Linear layers for query, key and value computation in a regular self-attention. Attention means a standard self-attention operator that works on local windows.

Window Token Embedding. A straightforward solution to model the attention relationship among windows is to employ all pixel tokens. However, it will bring huge computational costs and make the whole model very complicated.

To better establish the attention relationship among windows, we present a window token embedding scheme, which leverages a single token to encapsulate the core information for each sub-window. This window token can be initialized either as a fixed zero vector or a learnable vector with the initialization of zero. While passing through DWA, there is an informational interaction between the window token and pixel tokens in each window. Thus the window token can learn a global representation of this window. Thanks to the effective window token, we can model the attention relationship among windows with negligible computational cost.

Pointwise Self-Attention (PWA). The famous pointwise convolution in MobileNets is utilized to fuse the information from different channels. In our work, we imitate pointwise convolution to develop the pointwise self-attention (PWA) module to establish connections among windows. PWA is also mainly used to fuse the information across windows and obtain a final representation of the input feature map. More specifically, we extract the feature maps and window tokens from the output of DWA. Then, window tokens are used to model the attention relationship among windows and generate the attention map after a LayerNormalization (LN) layer and a Gelu activation function. Meanwhile, we directly treat the feature maps as the value branch of PWA without any other extra operation.

With the attention map and the feature maps which are in the form of windows, we perform an attention computation among the windows for global information exchange. Formally, the implementation of PWA can be depicted as follows:

$$\text{PWA}(z, wt) = \text{Attention}(\text{Gelu}(\text{LN}(wt)) \cdot W_Q, \text{Gelu}(\text{LN}(wt)) \cdot W_K, z) \quad (2)$$

where wt denotes the window token. Here, Attention is a standard self-attention operator but works on all of the windows z .

Complexity Analysis. Given an input feature with size $H \times W \times C$, the computational complexity of the multi-head self-attention (MSA) is $4HWC^2 + 2H^2W^2C$ in the global Transformer block of ViT [9]. The complexity of the MSA in a window-based Transformer with window size $M \times M$ (Usually, M is a common factor of H and W , so the number of the windows is $N = \frac{HW}{M^2}$) can be decreased to $4HWC^2 + 2M^2HWC$ in Swin [23]. As for the depthwise separable self-attention in SepViT, the complexity contains two parts, DWA and PWA.

DWA. Building on top of a window-based self-attention, DWA shares a similar computational cost to it. Additionally, the introduction of window tokens will cause an extra cost, but it is negligible compared to the overall cost of DWA. The complexity of DWA can be calculated as follows:

$$\Omega(\text{DWA}) = 3HWC^2 + 3NC^2 + 2N(M^2 + 1)^2C \quad (3)$$

where $3NC^2$ is the extra cost of encoding window tokens in Linear layers. $2N(M^2 + 1)^2C$ indicates the matrix multiplications involved in the self-attention

for N windows, where $M^2 + 1$ represents the M^2 pixel tokens in a window and its corresponding window token. Thanks to that the number of sub-windows N is usually a small value, the extra costs caused by window tokens can be ignored.

PWA. Since the window token summarizes the global information of a local window, the proposed PWA helps to efficiently perform information exchange among windows in a window level instead of pixel level. Concretely, the complexity of PWA is given as follows:

$$\Omega(\text{PWA}) = HWC^2 + 2NC^2 + N^2C + NHWC \quad (4)$$

where $2NC^2$ represents the little cost of computing the query and key with N window tokens, while the value branch is zero-cost. N^2C indicates the computation of generating attention map with N window tokens in a window level, which saves computational cost for PWA to a great extent. Finally, $NHWC$ indicates the matrix multiplication between the attention map and the feature maps.

3.3 Grouped Self-Attention

Motivated by the excellent performance of grouped convolution in visual recognition [19], we make an extension of our depthwise separable self-attention with the ideology of group, and propose the grouped self-attention. As shown in Fig. 3, we splice several neighboring sub-windows to form a larger window, which is similar to dividing the windows into groups and conducting a depthwise self-attention communication inside a group of windows. In this way, the grouped self-attention can capture long-range visual dependencies of multiple windows. In terms of computational cost and performance gains, the grouped self-attention has a certain extra cost compared with the depthwise separable self-attention but results in a better performance. Ultimately, we apply the block with grouped self-attention to SepViT and run it alternately with the depthwise separable self-attention block in the late stages of the network.

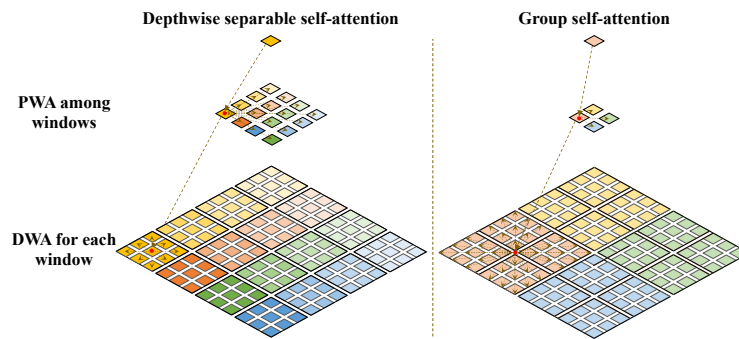


Fig. 3. A macro view of the similarities and differences between the depthwise separable self-attention and the grouped self-attention.

3.4 SepViT Block

To summarize, our SepViT block can be formulated as follows:

$$\tilde{z}^l = \text{Concat}(z^{l-1}, wt) \quad (5)$$

$$\ddot{z}^l = \text{DWA}(\text{LN}(\tilde{z}^l)) \quad (6)$$

$$\dot{z}^l, \dot{wt} = \text{Slice}(\ddot{z}^l) \quad (7)$$

$$\hat{z}^l = \text{PWA}(\dot{z}^l, \dot{wt}) + z^{l-1} \quad (8)$$

$$z^l = \text{MLP}(\text{LN}(\hat{z}^l)) + \hat{z}^l \quad (9)$$

where \tilde{z}^l , \ddot{z}^l and \hat{z}^l denote the outputs of the DWA, PWA and SepViT block l , respectively. \dot{z}^l and \dot{wt} are feature maps and the learned window tokens. Concat represents the concatenation operation while Slice represents the slice operation.

Comparison of Complexity. We compare the complexity of our proposed SepViT block with two other SOTA blocks (Swin [23], Twins [5]). As we stated before, the information interaction within and among windows is completed in a single SepViT block, while Swin [23] and Twins [5] require two successive blocks. As shown in Fig. 4, we can observe that the SepViT block only costs about half the MACs of its competitors in each stage of the network. The reason lies in two aspects: i) SepViT block is more lightweight; ii) SepViT block removes many redundant layers, e.g., there is only one MLP layer and two LN layers in a single SepViT block while there are double MLP and LN layers in two successive Swin or Twins blocks.

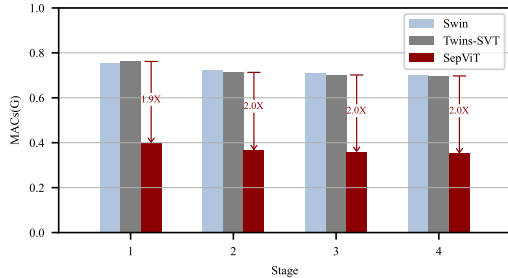


Fig. 4. Complexity comparison of an information interaction within and among windows in a single SepViT block with those two-block pattern works in each stage.

3.5 Architecture Configurations

To provide a fair comparison with other vision Transformers, we propose the SepViT-T (Tiny), SepViT-S (Small) and SepViT-B (Base) variants. Moreover,

Table 1. Detailed configurations of SepViT variants in different stages.

Configuration	SepViT-Lite	SepViT-T	SepViT-S	SepViT-B
Blocks	[1, 2, 6, 2]	[1, 2, 6, 2]	[1, 2, 14, 2]	[1, 2, 14, 2]
Channels	[32, 64, 128, 256]	[96, 192, 384, 768]	[96, 192, 384, 768]	[128, 256, 512, 1024]
Heads	[1, 2, 4, 8]	[3, 6, 12, 24]	[3, 6, 12, 24]	[4, 8, 16, 32]
Block Type	[DSSA, DSSA&GSA, DSSA&GSA, DSSA]			

we also design the SepViT-Lite variant with a very light model size. The specific configurations of SepViT variants are shown in Table 1, the block depth of SepViT is smaller in some stages than the competitors since SepViT is more efficient. DSSA and GSA denote the blocks with depthwise separable self-attention and grouped self-attention, respectively. Additionally, the expansion ratio of each MLP layer is set as 4, the window sizes are 7×7 and 14×14 for DSSA and GSA in all SepViT variants.

4 Experimental Results

4.1 ImageNet-1K Classification

Settings. We carry out the image classification experiment on the ImageNet-1K [28], which contains about 1.28M training images and 50K validation images from 1K categories. For a fair comparison, we follow the training settings of the recent vision Transformer [5]. Concretely, all of the SepViT variants are trained for 300 epochs on 8 V100 GPUs with a total batch size of 1024. The resolution of the input image is resized to 224×224 . We adopt the AdamW [24] as the optimizer with weight decay 0.1 for SepViT-B and 0.05 for SepViT-S/T. The learning rate is gradually decayed based on the cosine strategy with the initialization of 0.001. We use a linear warm-up strategy with 20 epochs for SepViT-B and 5 epochs for SepViT-S/T. Besides, we have also employed the increasing stochastic depth augmentation [17] with the maximum drop-path rate of 0.2, 0.3, 0.5 for our SepViT-T/S/B models.

Results. As shown in Table 2, compared to the latest state-of-the-art methods, our SepViT achieves the best trade-off between accuracy and latency. To be more specific, our SepViT-B and SepViT-S achieve 84.0% and 83.5% top-1 accuracy, surpassing Swin by 0.7% and 0.5% with about 14% fewer FLOPs. And for the tiny variant, our SepViT-T outperforms the Swin-T by 1.2% with the same FLOPs of 4.5G. In terms of latency, compared to the recent methods (e.g., PVT-v2 [34] and CSWin [8]) with similar performance, both of our small and base models cost about 40% less inference time. Moreover, our SepViT shows very promising performance by comparison with the CNNs counterparts.

Table 2. Comparison of different state-of-the-art methods on ImageNet-1K classification. Throughput and latency are tested based on the PyTorch framework with a V100 GPU (batchsize=192) and TensorRT framework with a T4 GPU (batchsize=8).

Method	Param FLOPs		Throughput (Images/s)	Latency (ms)	Top-1 Acc (%)
	(M)	(G)			
ConvNet					
RegNetY-4G[27]	21.0	4.0	1064	-	80.0
RegNetY-8G[27]	39.0	8.0	548	-	81.7
RegNetY-16G[27]	84.0	16.0	305	-	82.9
Transformer					
DeiT-Small/16[32]	22.0	4.6	406	-	79.9
T2T-ViT-14[42]	22.0	5.2	-	-	81.5
TNT-S[12]	23.8	5.2	-	-	81.3
CoaT-Lite-Small[40]	20.0	4.0	-	-	81.9
CvT-13[36]	20.0	4.5	-	-	81.6
PVT-Small[35]	24.5	3.8	794	20.7	79.8
Swin-T[23]	29.0	4.5	704	-	81.3
Twins-PCPVT-S[5]	24.1	3.8	778	20.2	81.7
Twins-SVT-S[5]	24.0	2.9	979	18.8	81.7
CSWin-T[8]	23.0	4.3	627	30.2	82.7
PVT-v2-B2[34]	25.4	4.0	664	37.8	82.0
SepViT-T	31.2	4.5	738	23.7	82.5
T2T-ViT-19[42]	39.2	8.9	-	-	81.9
CoaT-Lite-Medium[40]	45.0	9.8	-	-	83.6
CvT-21[36]	32.0	7.1	-	-	82.5
PVT-Medium[35]	44.2	6.7	511	30.0	81.2
Swin-S[23]	50.0	8.7	412	-	83.0
Twins-PCPVT-B[5]	43.8	6.7	502	29.1	82.7
Twins-SVT-B[5]	56.0	8.6	433	38.9	83.2
CSWin-S[8]	35.0	6.9	390	52.0	83.6
PVT-v2-B3[34]	45.2	6.9	443	54.1	83.2
SepViT-S	46.6	7.5	476	34.5	83.5
DeiT-Base/16[32]	86.6	17.6	273	-	81.8
T2T-ViT-24[42]	64.1	14.1	-	-	82.3
TNT-B[12]	66.0	14.1	-	-	82.8
PVT-Large[35]	61.4	9.8	357	43.2	81.7
Swin-B[23]	88.0	15.4	255	-	83.3
Twins-PCPVT-L[5]	60.9	9.8	339	39.8	83.1
Twins-SVT-L[5]	99.2	15.1	271	48.3	83.7
CSWin-B[8]	78.0	15.0	216	76.1	84.2
PVT-v2-B4[34]	62.6	10.1	298	75.5	83.6
PVT-v2-B5[34]	82.0	11.8	285	77.5	83.8
SepViT-B	82.3	13.1	308	46.0	84.0

4.2 ADE20K Semantic Segmentation

Settings. To further verify the capacity of our SepViT, we conduct the semantic segmentation experiment on ADE20K [45], which contains about 20K training images and 2K validation images from 150 categories. To make fair comparisons, we also follow the training conventions of the previous vision Transformers [35,23,5] on the Semantic FPN [18] and UperNet [37] frameworks. All of our models are pre-trained on the ImageNet-1k and then finetuned on ADE20K with the input size of 512×512 . For the Semantic FPN framework, we adopt the AdamW optimizer with both the learning rate and weight decay being 0.0001. Then we train the whole networks for 80K iterations with the total batch size of 16 based on the stochastic depth of 0.2, 0.3, and 0.4 for SepViT-T/S/B. For the training and testing on the UperNet framework, we train the models for 160K

Table 3. Comparison of different backbones on ADE20K semantic segmentation task. FLOPs are measured with the input size of 512×2048 .

Backbone	Semantic FPN 80k			UperNet 160k		
	Param(M)	FLOPs(G)	mIoU(%)	Param(M)	FLOPs(G)	mIoU/MS mIoU(%)
ResNet50[14]	28.5	183	36.7	-	-	-/-
PVT-Small[35]	28.2	161	39.8	-	-	-/-
Swin-T[23]	31.9	182	41.5	59.9	945	44.5/45.8
Twins-PCPVT-S[5]	28.4	162	44.3	54.6	919	46.2/47.5
Twins-SVT-S[5]	28.3	144	43.2	54.4	901	46.2/47.1
SepViT-T	38.8	181	44.3	66.8	940	46.9/47.7
ResNet101[14]	47.5	260	38.8	86.0	1092	-/44.9
PVT-Medium[35]	48.0	219	41.6	-	-	-/-
Swin-S[23]	53.2	274	45.2	81.3	1038	47.6/ 49.5
Twins-PCPVT-B[5]	48.1	220	44.9	74.3	977	47.1/48.4
Twins-SVT-B[5]	60.4	261	45.3	88.5	1020	47.7/48.9
SepViT-S	55.4	244	46.1	83.4	1003	48.1/49.2
ResNeXt101-64 \times 4d[39]	86.4	-	40.2	-	-	-/-
PVT-Large[35]	65.1	283	42.1	-	-	-/-
Swin-B[23]	91.2	422	46.0	121.0	1188	48.1/49.7
Twins-PCPVT-L[5]	65.3	283	46.4	91.5	1041	48.6/49.8
Twins-SVT-L[5]	103.7	404	46.7	133.0	1164	48.8/49.7
SepViT-B	94.7	367	47.3	124.8	1128	49.1/50.4

iterations with the stochastic depth of 0.3, 0.3, and 0.5. AdamW optimizer is used as well but with the learning rate 6×10^{-5} , total batch size 16 and weight decay 0.01 for SepViT-T/S and 0.03 for SepViT-B. Then we test the mIoU based on both single-scale and multi-scale (MS) where the scale goes from 0.5 to 1.75 with an interval of 0.25.

Results. In Table 3, we make a comparison with the recent vision Transformer and CNN backbones. Based on the Semantic FPN framework, SepViT-T, SepViT-S and SepViT-B surpass Swin’s variants by 2.8%, 0.9% and 1.3% mIoU with about 1G, 30G and 55G fewer FLOPs, respectively. Meanwhile, our SepViT shows great advantage over CNNs (e.g., ResNet[14]). By contrast to Swin on the UperNet framework, our models achieve 2.4%, 0.5% and 1.0% higher mIoU with fewer FLOPs in terms of single-scale testing. Extensive experiments reveal that our SepViT shows great potential on segmentation tasks.

4.3 COCO Object Detection and Instance Segmentation

Settings. Next, we evaluate SepViT on the objection detection and instance segmentation task [22] based the RetinaNet [21] and Mask R-CNN [13] frameworks with COCO2017 [22]. Specifically, all of our models are pre-trained on ImageNet-1K and then finetuned following the settings of the previous works [35,23,5]. As for the 12 epochs ($1 \times$) experiment, both the RetinaNet-based and the Mask R-CNN-based models use the AdamW optimizer with the weight decay 0.001 for SepViT-T and 0.0001 for SepViT-S. And they are trained with the total batch size of 16 based on the stochastic depth of 0.2 and 0.3 for SepViT-T/S. During the training, there are 500 iterations for warm-up and the learning

Table 4. Comparison of different backbones on RetinaNet-based object detection task. FLOPs are measured with the input size of 800×1280 .

Backbone	Param FLOPs		RetinaNet 1×						RetinaNet 3× + MS					
	(M)	(G)	AP	AP ₅₀	AP ₇₅	AP _S	AP _M	AP _L	AP	AP ₅₀	AP ₇₅	AP _S	AP _M	AP _L
ResNet50[14]	37.7	239	36.3	55.3	38.6	19.3	40.0	48.8	39.0	58.4	41.8	22.4	42.8	51.6
PVT-Small[35]	34.2	226	40.4	61.3	43.0	25.0	42.9	55.7	42.2	62.7	45.0	26.2	45.2	57.2
Swin-T[23]	38.5	245	41.5	62.1	44.2	25.1	44.9	55.5	43.9	64.8	47.1	28.4	47.2	57.8
Twins-PCPVT-S[5]	34.4	226	43.0	64.1	46.0	27.5	46.3	57.3	45.2	66.5	48.6	30.0	48.8	58.9
Twins-SVT-S[5]	34.4	210	43.0	64.2	46.3	28.0	46.4	57.5	45.6	67.1	48.6	29.8	49.3	60.0
SepViT-T	45.4	243	43.9	65.1	46.2	28.4	47.3	58.5	46.2	67.7	49.4	30.3	49.8	60.7
ResNet101[14]	58.0	315	38.5	57.8	41.2	21.4	42.6	51.1	40.9	60.1	44.0	23.7	45.0	53.8
PVT-Medium[35]	53.9	283	41.9	63.1	44.3	25.0	44.9	57.6	43.2	63.8	46.1	27.3	46.3	58.9
Swin-S[23]	59.8	335	44.5	65.7	47.5	27.4	48.0	59.9	46.3	67.4	49.8	31.1	50.3	60.9
Twins-PCPVT-S[5]	54.1	283	44.3	65.6	47.3	27.9	47.9	59.6	46.4	67.7	49.8	31.3	50.2	61.4
Twins-SVT-B[5]	67.0	326	45.3	66.7	48.1	28.5	48.9	60.6	46.9	68.0	50.2	31.7	50.3	61.8
SepViT-S	61.9	302	45.5	66.8	48.3	28.9	49.4	60.8	47.5	68.9	50.9	32.4	51.1	62.5

Table 5. Comparison of different backbones on Mask R-CNN-based object detection and instance segmentation tasks. FLOPs are measured with the input size of 800×1280 . The superscript b and m denote the box detection and mask instance segmentation.

Backbone	Param FLOPs		Mask R-CNN 1×						Mask R-CNN 3× + MS					
	(M)	(G)	AP ^b	AP ₅₀ ^b	AP ₇₅ ^b	AP ^m	AP ₅₀ ^m	AP ₇₅ ^m	AP ^b	AP ₅₀ ^b	AP ₇₅ ^b	AP ^m	AP ₅₀ ^m	AP ₇₅ ^m
ResNet50[14]	44.2	260	38.0	58.6	41.4	34.4	55.1	36.7	41.0	61.7	44.9	37.1	58.4	40.1
PVT-Small[35]	44.1	245	40.4	62.9	43.8	37.8	60.1	40.3	43.0	65.3	46.9	39.9	62.5	42.8
Swin-T[23]	47.8	264	42.2	64.4	46.2	39.1	64.6	42.0	46.0	68.2	50.2	41.6	65.1	44.8
Twins-PCPVT-S[5]	44.0	245	42.9	65.8	47.1	40.0	62.7	42.9	46.8	69.3	51.8	42.6	66.3	46.0
Twins-SVT-S[5]	44.0	228	43.4	66.0	47.3	40.3	63.2	43.4	46.8	69.2	51.2	42.6	66.3	45.8
SepViT-T	54.7	261	44.4	67.1	48.3	41.1	64.1	43.9	47.5	70.0	52.3	43.2	67.1	46.3
ResNet101[14]	63.2	336	40.4	61.1	44.2	36.4	57.7	38.8	42.8	63.2	47.1	38.5	60.1	41.3
ResNeXt101-32×4d[39]	63.0	340	41.9	62.5	45.9	37.5	59.4	40.2	44.0	64.4	48.0	39.2	61.4	41.9
PVT-Medium[35]	63.9	302	42.0	64.4	45.6	39.0	61.6	42.1	44.2	66.0	48.2	40.5	63.1	43.5
Swin-S[23]	69.1	354	44.8	66.6	48.9	40.9	63.4	44.2	48.5	70.2	53.5	43.3	67.3	46.6
Twins-PCPVT-B[5]	64.0	302	44.6	66.7	48.9	40.9	63.8	44.2	47.9	70.1	52.5	43.2	67.2	46.3
Twins-SVT-B[5]	76.3	340	45.2	67.6	49.3	41.5	64.5	44.8	48.0	69.5	52.7	43.0	66.8	46.6
SepViT-S	71.3	321	46.3	68.0	49.8	42.3	65.8	45.3	48.7	70.5	53.7	43.9	67.7	47.1

rate will decline by 10× at epochs 8 and 11. For the 36 epochs (3×) experiment with multi-scale (MS) training, models are trained with the resized images such that the shorter side ranges from 480 to 800 and the longer side is at most 1333. Moreover, most of all the other settings are the same as the 1× except that the stochastic depth is 0.3 for SepViT-T, the weight decay becomes 0.05 and 0.1 for SepViT-T/S, and the decay epochs are 27 and 33.

Results. Table 4 reports object detection results using the RetinaNet framework. It indicates that our SepViT can achieve competitive performance, compared with the recent vision Transformers and CNNs. For the 1× schedule, our SepViT-T and SepViT-S surpass the Swin by 2.4 AP and 1.0 AP with fewer FLOPs. In particular, our SepViT variants achieve a state-of-the-art performance with 46.2 AP and 47.5 AP in the 3× experiment. Table 5 shows the evaluation result with Mask R-CNN framework. We can see that our SepViT-T outperforms Swin-T by 2.2 box AP, 2.0 mask AP with 1× schedule, and 1.5 box

Table 6. Ablation studies of the key components in our SepViT. LWT means initializing the window tokens with learnable vectors.

Model	DSSA	GSA	LWT	Param(M)	FLOPs(G)	Throughput(Images/s)	Top-1 Acc(%)
Swin-T+CPVT [5]				28.0	4.4	704	81.2
SepViT-T†	✓			29.3	4.3	755	81.7
SepViT-T	✓			32.1	4.4	746	82.0
	✓	✓		31.2	4.5	738	82.3
	✓	✓	✓	31.2	4.5	738	82.5

AP, 1.6 mask AP with $3\times$ schedule. For the SepViT-S variant, it achieves a similar performance gain while saving a certain amount of computation overhead.

4.4 Ablation Study

To better demonstrate the significance of each key component, including depthwise separable self-attention, grouped self-attention and the novel window token embedding scheme in SepViT, we conduct a series of ablation experiments on ImageNet-1K classification with SepViT-T variant.

Efficient Components. As mentioned above, SepViT adopts the conditional position encoding (CPE) [6] and the overlapping patch embedding (OPE) [9]. Therefore, we take the Swin-T+CPVT reported in [5] as the baseline and we produce the SepViT-T† with CPE but without OPE to eliminate the influence of other factors. As shown in Table 6 where each component is added in turn to verify their benefits, our SepViT-T† simply equipped with the depthwise separable self-attention block (DSSA) outperforms Swin+CPVT by 0.5% and it is much faster than Swin with the throughput of 755 images/s. Meanwhile, our SepViT-T with CPE, OPE and DSSA achieves 82.0% top-1 accuracy. After employing grouped self-attention block (GSA) and DSSA alternately in the second and third stages, we gain an accuracy improvement of 0.3%.

Window Token Embedding. We further study whether it makes a difference if the window token is initialized with a fixed zero vector or a learnable vector. In contrast to the fixed zero initialization scheme, the learnable window token helps our SepViT-T to boost the performance to 82.5%, as shown in the last row of Table 6.

Table 7. Comparison of different approaches of getting the global representation of each window in SepViT.

Method	Param(M)	FLOPs(G)	Throughput(Images/s)	Top-1 Acc(%)
Win_Tokens	31.2	4.5	738	82.5
Avg_Pooling	31.2	4.5	743	82.1
Dw_Conv	31.3	4.5	735	82.3

Table 8. Comparison of lite models on ImageNet-1K classification.

Method	Param(M)	FLOPs(G)	Top-1 Acc(%)
MobileNet-V2 [29]	3.4	0.3	71.8
ResNet18 [14]	11.1	1.8	69.8
PVTv2-B0 [34]	3.4	0.6	70.5
SepViT-Lite	3.7	0.6	72.3

Moreover, to verify the effectiveness of learning the global representation of each window with our window token embedding scheme (Win_Tokens), we further study some other methods that directly get the global representations from the output feature maps of DWA, such as average pooling (Avg_Pooling) and depthwise convolution (DW_Conv). As the results illustrated in Table 7, our window token embedding scheme achieves the best performance among these approaches. Meanwhile, the comparison of parameters and FLOPs between Win-Token and Avg_Pooling methods demonstrates that our window token embedding scheme brings negligible computational cost.

Comparison with Lite Models. To further explore the potential of SepViT, we scale down SepViT to a lite model size (SepViT-Lite). As we can observe in Table 8, SepViT-Lite obtains an excellent top-1 accuracy of 72.3%, outperforming its counterparts with similar model sizes.

5 Conclusion

In this paper, we have presented an efficient Separable Vision Transformer, dubbed SepViT, which consists of three core designs. Firstly, depthwise separable self-attention enables SepViT to achieve information interaction within and among the windows in a single block. Next, the window token embedding scheme helps SepViT to model the attention relationship among windows with negligible computational cost. Thirdly, grouped self-attention enables SepViT to capture long-range visual dependencies across multiple windows for better performance. Experimental results on various vision tasks verify that SepViT achieves a better trade-off between performance and latency.

References

1. Carion, N., Massa, F., Synnaeve, G., Usunier, N., Kirillov, A., Zagoruyko, S.: End-to-end object detection with transformers. In: European Conference on Computer Vision. pp. 213–229 (2020)
2. Chen, B., Li, P., Li, C., Li, B., Bai, L., Lin, C., Sun, M., Yan, J., Ouyang, W.: Glit: Neural architecture search for global and local image transformer. In: Proceedings of the IEEE/CVF International Conference on Computer Vision. pp. 12–21 (2021)

3. Chen, M., Peng, H., Fu, J., Ling, H.: Autoformer: Searching transformers for visual recognition. In: Proceedings of the IEEE/CVF International Conference on Computer Vision. pp. 12270–12280 (2021)
4. Chen, Y., Dai, X., Chen, D., Liu, M., Dong, X., Yuan, L., Liu, Z.: Mobile-former: Bridging mobilenet and transformer. arXiv preprint arXiv:2108.05895 (2021)
5. Chu, X., Tian, Z., Wang, Y., Zhang, B., Ren, H., Wei, X., Xia, H., Shen, C.: Twins: Revisiting the design of spatial attention in vision transformers. arXiv preprint arXiv:2104.13840 (2021)
6. Chu, X., Tian, Z., Zhang, B., Wang, X., Wei, X., Xia, H., Shen, C.: Conditional positional encodings for vision transformers. arXiv preprint arXiv:2102.10882 (2021)
7. Dai, Z., Cai, B., Lin, Y., Chen, J.: Up-detr: Unsupervised pre-training for object detection with transformers. In: Proceedings of the IEEE/CVF Conference on Computer Vision and Pattern Recognition. pp. 1601–1610 (2021)
8. Dong, X., Bao, J., Chen, D., Zhang, W., Yu, N., Yuan, L., Chen, D., Guo, B.: Cswin transformer: A general vision transformer backbone with cross-shaped windows. arXiv preprint arXiv:2107.00652 (2021)
9. Dosovitskiy, A., Beyer, L., Kolesnikov, A., Weissenborn, D., Zhai, X., Unterthiner, T., Dehghani, M., Minderer, M., Heigold, G., Gelly, S., et al.: An image is worth 16x16 words: Transformers for image recognition at scale. arXiv preprint arXiv:2010.11929 (2020)
10. Graham, B., El-Nouby, A., Touvron, H., Stock, P., Joulin, A., Jégou, H., Douze, M.: Levit: a vision transformer in convnet’s clothing for faster inference. In: Proceedings of the IEEE/CVF International Conference on Computer Vision. pp. 12259–12269 (2021)
11. Han, K., Wang, Y., Tian, Q., Guo, J., Xu, C., Xu, C.: Ghostnet: More features from cheap operations. In: Proceedings of the IEEE/CVF Conference on Computer Vision and Pattern Recognition. pp. 1580–1589 (2020)
12. Han, K., Xiao, A., Wu, E., Guo, J., Xu, C., Wang, Y.: Transformer in transformer. Advances in Neural Information Processing Systems **34** (2021)
13. He, K., Gkioxari, G., Dollár, P., Girshick, R.: Mask r-cnn. In: Proceedings of the IEEE International Conference on Computer Vision. pp. 2961–2969 (2017)
14. He, K., Zhang, X., Ren, S., Sun, J.: Deep residual learning for image recognition. In: Proceedings of the IEEE Conference on Computer Vision and Pattern Recognition. pp. 770–778 (2016)
15. Howard, A., Sandler, M., Chu, G., Chen, L.C., Chen, B., Tan, M., Wang, W., Zhu, Y., Pang, R., Vasudevan, V., et al.: Searching for mobilenetv3. In: Proceedings of the IEEE/CVF International Conference on Computer Vision. pp. 1314–1324 (2019)
16. Howard, A.G., Zhu, M., Chen, B., Kalenichenko, D., Wang, W., Weyand, T., Andreetto, M., Adam, H.: Mobilenets: Efficient convolutional neural networks for mobile vision applications. arXiv preprint arXiv:1704.04861 (2017)
17. Huang, G., Sun, Y., Liu, Z., Sedra, D., Weinberger, K.Q.: Deep networks with stochastic depth. In: European Conference on Computer Vision. pp. 646–661 (2016)
18. Kirillov, A., Girshick, R., He, K., Dollár, P.: Panoptic feature pyramid networks. In: Proceedings of the IEEE/CVF Conference on Computer Vision and Pattern Recognition. pp. 6399–6408 (2019)
19. Krizhevsky, A., Sutskever, I., Hinton, G.E.: Imagenet classification with deep convolutional neural networks. Advances in Neural Information Processing Systems **25** (2012)

20. Li, C., Tang, T., Wang, G., Peng, J., Wang, B., Liang, X., Chang, X.: Bossnas: Exploring hybrid cnn-transformers with block-wisely self-supervised neural architecture search. In: Proceedings of the IEEE/CVF International Conference on Computer Vision. pp. 12281–12291 (2021)
21. Lin, T.Y., Goyal, P., Girshick, R., He, K., Dollár, P.: Focal loss for dense object detection. In: Proceedings of the IEEE International Conference on Computer Vision. pp. 2980–2988 (2017)
22. Lin, T.Y., Maire, M., Belongie, S., Hays, J., Perona, P., Ramanan, D., Dollár, P., Zitnick, C.L.: Microsoft coco: Common objects in context. In: European Conference on Computer Vision. pp. 740–755 (2014)
23. Liu, Z., Lin, Y., Cao, Y., Hu, H., Wei, Y., Zhang, Z., Lin, S., Guo, B.: Swin transformer: Hierarchical vision transformer using shifted windows. arXiv preprint arXiv:2103.14030 (2021)
24. Loshchilov, I., Hutter, F.: Decoupled weight decay regularization. arXiv preprint arXiv:1711.05101 (2017)
25. Ma, N., Zhang, X., Zheng, H.T., Sun, J.: Shufflenet v2: Practical guidelines for efficient cnn architecture design. In: Proceedings of the European Conference on Computer Vision. pp. 116–131 (2018)
26. Mehta, S., Rastegari, M.: Mobilevit: light-weight, general-purpose, and mobile-friendly vision transformer. arXiv preprint arXiv:2110.02178 (2021)
27. Radosavovic, I., Kosaraju, R.P., Girshick, R., He, K., Dollár, P.: Designing network design spaces. In: Proceedings of the IEEE/CVF Conference on Computer Vision and Pattern Recognition. pp. 10428–10436 (2020)
28. Russakovsky, O., Deng, J., Su, H., Krause, J., Satheesh, S., Ma, S., Huang, Z., Karpathy, A., Khosla, A., Bernstein, M., et al.: Imagenet large scale visual recognition challenge. *International Journal of Computer Vision* **115**(3), 211–252 (2015)
29. Sandler, M., Howard, A., Zhu, M., Zhmoginov, A., Chen, L.C.: Mobilenetv2: Inverted residuals and linear bottlenecks. In: Proceedings of the IEEE Conference on Computer Vision and Pattern Recognition. pp. 4510–4520 (2018)
30. So, D., Le, Q., Liang, C.: The evolved transformer. In: International Conference on Machine Learning. pp. 5877–5886 (2019)
31. Tan, M., Le, Q.: Efficientnet: Rethinking model scaling for convolutional neural networks. In: International Conference on Machine Learning. pp. 6105–6114 (2019)
32. Touvron, H., Cord, M., Douze, M., Massa, F., Sablayrolles, A., Jégou, H.: Training data-efficient image transformers & distillation through attention. In: International Conference on Machine Learning. pp. 10347–10357 (2021)
33. Wang, H., Zhu, Y., Adam, H., Yuille, A., Chen, L.C.: Max-deeplab: End-to-end panoptic segmentation with mask transformers. In: Proceedings of the IEEE/CVF Conference on Computer Vision and Pattern Recognition. pp. 5463–5474 (2021)
34. Wang, W., Xie, E., Li, X., Fan, D.P., Song, K., Liang, D., Lu, T., Luo, P., Shao, L.: Pvtv2: Improved baselines with pyramid vision transformer. arXiv preprint arXiv:2106.13797 (2021)
35. Wang, W., Xie, E., Li, X., Fan, D.P., Song, K., Liang, D., Lu, T., Luo, P., Shao, L.: Pyramid vision transformer: A versatile backbone for dense prediction without convolutions. arXiv preprint arXiv:2102.12122 (2021)
36. Wu, H., Xiao, B., Codella, N., Liu, M., Dai, X., Yuan, L., Zhang, L.: Cvt: Introducing convolutions to vision transformers. In: Proceedings of the IEEE/CVF International Conference on Computer Vision. pp. 22–31 (2021)
37. Xiao, T., Liu, Y., Zhou, B., Jiang, Y., Sun, J.: Unified perceptual parsing for scene understanding. In: European Conference on Computer Vision. pp. 418–434 (2018)

38. Xie, E., Wang, W., Yu, Z., Anandkumar, A., Alvarez, J.M., Luo, P.: Segformer: Simple and efficient design for semantic segmentation with transformers. *Advances in Neural Information Processing Systems* **34** (2021)
39. Xie, S., Girshick, R., Dollár, P., Tu, Z., He, K.: Aggregated residual transformations for deep neural networks. In: *Proceedings of the IEEE Conference on Computer Vision and Pattern Recognition*. pp. 1492–1500 (2017)
40. Xu, W., Xu, Y., Chang, T., Tu, Z.: Co-scale conv-attentional image transformers. In: *Proceedings of the IEEE/CVF International Conference on Computer Vision*. pp. 9981–9990 (2021)
41. Yu, J., Jin, P., Liu, H., Bender, G., Kindermans, P.J., Tan, M., Huang, T., Song, X., Pang, R., Le, Q.: Bignas: Scaling up neural architecture search with big single-stage models. In: *European Conference on Computer Vision*. pp. 702–717 (2020)
42. Yuan, L., Chen, Y., Wang, T., Yu, W., Shi, Y., Jiang, Z.H., Tay, F.E., Feng, J., Yan, S.: Tokens-to-token vit: Training vision transformers from scratch on imagenet. In: *Proceedings of the IEEE/CVF International Conference on Computer Vision*. pp. 558–567 (2021)
43. Zhang, X., Zhou, X., Lin, M., Sun, J.: Shufflenet: An extremely efficient convolutional neural network for mobile devices. In: *Proceedings of the IEEE Conference on Computer Vision and Pattern Recognition*. pp. 6848–6856 (2018)
44. Zheng, S., Lu, J., Zhao, H., Zhu, X., Luo, Z., Wang, Y., Fu, Y., Feng, J., Xiang, T., Torr, P.H., et al.: Rethinking semantic segmentation from a sequence-to-sequence perspective with transformers. In: *Proceedings of the IEEE/CVF Conference on Computer Vision and Pattern Recognition*. pp. 6881–6890 (2021)
45. Zhou, B., Zhao, H., Puig, X., Fidler, S., Barriuso, A., Torralba, A.: Scene parsing through ade20k dataset. In: *Proceedings of the IEEE Conference on Computer Vision and Pattern Recognition*. pp. 633–641 (2017)
46. Zhu, X., Su, W., Lu, L., Li, B., Wang, X., Dai, J.: Deformable detr: Deformable transformers for end-to-end object detection. *arXiv preprint arXiv:2010.04159* (2020)
47. Zoph, B., Le, Q.V.: Neural architecture search with reinforcement learning. *arXiv preprint arXiv:1611.01578* (2016)